The Numerical Simulation of Fatigue Crack Propagation in Inconel 718 Alloy at Different Temperatures

C. Duan[1], X. H. Chen[1*]

1School of Aeronautics and Astronautics, Shanghai Jiao Tong University, Shanghai, P.R. China, 200240

* Corresponding author (Tel: +86-13774386981, E-Mail: chenxiuhua@sjtu.edu.cn)

Abstract: Inconel718 alloy is the most commonly used material of aero-engine turbine today. However, Inconel718 alloy is known to suffer from the fatigue crack propagation during engine operation, which will lead to unstable fracture and seriously threatens the safety of the engine. In this paper, we research the fatigue crack propagation process of Inconel718 alloy unilateral notched standard CT specimen at room temperature(298.15K), 573.15K and 823.15K under the type I cyclic fatigue load. The ABAQUS is used for numerical simulation. First, parametric models are established. Second, the extended finite element method (XFEM) is used to output the PHILSM function and the PSILSM function in the calculation process for describing the crack state. Third, the stress intensity factor at the crack tip under different temperatures is calculated, and the extended finite element crack length is solved to obtain the fatigue crack growth rate da/dN curve. The results show that the simulated fatigue crack growth rate da/dN curve is basically consistent with the test results under the same conditions. Therefore the method reported in this paper can provide some reference for fatigue experiments.

Keywords: Inconel718; Fatigue crack propagation; numerical simulation; ABAQUS；XFEM

1 Introduction

As an excellent nickel-based alloy, Inconel718 is commonly used in aero-engine turbine disks and installation sections. In the process of aero-engine's work, The material must withstand the cyclic load, so it is easy to initiate fatigue cracks. If the fatigue crack is not treated well, it will gradually expand and seriously threatens the safety of the engine and aviation safety[1]. The Airworthiness also clearly states that damage tolerance assessments are required for critical load-bearing components. Therefore, studying the fatigue crack propagation behavior of Inconel718 alloy at different temperatures is of great significance for evaluating the damage tolerance and aviation safety.

As the fatigue test is costly, and numerical simulation links theory with practice, can certain guiding engineering practice at a small cost, By using the three-dimensional finite element method to calculate the stress intensity factor at a set of points on the crack front, the fatigue expansion analysis of various cracks can be reliably performed[2]. Characterizing elastoplastic fatigue crack propagation (EPFCG) by crack propagation analysis in advance is verified with experiments[3]. A three-dimensional cohesive element was developed to track the three-dimensional fatigue crack front[4]. At present, the methods of simulating crack propagation mainly include Boundary Element Method (BEM)[5], Mesh-less Method[6], Finite Difference Method (FDM), and Finite Element Method (FEM). However, when simulating dynamic crack propagation by them, the mesh needs to be continuously updated in the crack propagation process, it's almost impossible to realize the dynamic expansion of fatigue cracks by traditional methods.

The extended finite element method (XFEM) has been widely used in recent studies. XFEM was first proposed by belytschko and black in 1999[7]. It is based on the standard finite element framework and uses a special displacement function to allow the existence of discontinuities, overcome the need to continuously re-mesh during crack tip expansion process. XFEM were used to calculate SIF, performed crack growth analysis without updating the mesh[8].The fatigue crack propagation of interface cracks in two-layer materials were studied by using XFEM[9], as well as various three-dimensional planes, non-planar and arbitrary shapes fatigue crack propagation simulation[10]. Homogenized XFEM method is proposed to evaluate the fatigue life of edge-fractured plates in the presence of discontinuities[11]. J-integration and XFEM were used to simulate fatigue crack propagation in functionally graded materials/ plastic gradient materials, problem of fatigue crack growth in an aero-engine turbine disk made of a plastic graded material is solved[12].

Although the research work of the above literatures shows that XFEM has certain feasibility and accuracy in solving practical engineering problems. Nevertheless, there are few reports on the fatigue life prediction of XFEM in Nickel based superalloy, and the results obtained by XFEM still cannot be separated from the experimental results. The

main purpose of this paper is to use XFEM to analyze and simulate the fatigue crack growth process at room

temperature, 300 degree and 550 degrees under the type I cyclic fatigue load of Inconel718 unilateral notched standard CT specimens.In the calculation process, PHILSM and PSILSM are output to describe the crack state, the crack tip stress intensity factor at different temperatures is calculated, and the extended finite element crack length is solved to obtain the fatigue crack growth rate da/dN curve, which is confirmed by comparison with experimental results. The effectiveness of XFEM provides a basis for further engineering applications.

2 Extended finite element method theory

The extended finite element method (XFEM) is a numerical method for analyzing discontinuous problems based on the Unit Decomposition Method and the Level Set Method.

The basic idea of the Unit Decomposition Method is that any function in the domain can be represented by a set of local functions:

$$\psi(x) = \sum_i N_i(x)\phi_i(x) \tag{1}$$

Where $N_i(x)$ is an interpolation shape function, which forms a unit decomposition, any point in the domain x interpolation shape function should satisfy:

$$\sum_i N_i(x) = 1 \tag{2}$$

Based on the idea of unit decomposition method, the displacement function expression can be modified as needed, additional functions added to reflect local characteristics, and local discontinuity characteristics are indirectly simulated. In XFEM, the displacement approximate solution can be written as:

$$u^h(x) = \sum_i N_i(x)\left[\sum_j \psi_j(x)a_i^j\right] \tag{3}$$

Where $\psi_j(x)$ is an improved function, and the shape function still constitutes a unit decomposition:

$$\sum_i N_i(x) = 1 \tag{4}$$

The Level Set Method proposed by Sethian and Osher[13] can determine crack propagation interface position and track it's movement without re-meshing, it greatly reduces the computational cost. In order to get the crack position, two level set functions $\psi(x)$ and $\phi(x)$ are introduced. As shown in Figure 1, $\psi(x)$ is the distance function of the crack path or the crack surface, indicating the shortest distance from any point to the crack path or crack surface, specifying that $\psi(x) > 0$ above the crack; $\psi(x) < 0$ below the crack; $\psi(x) = 0$ on the crack surface. $\phi(x)$ is the distance function of the crack tip normal plane, indicates the shortest distance from any point to the crack path or the front plane of the crack. specifying that $\phi(x) > 0$ in front of the crack; $\phi(x) < 0$ behind the crack; $\phi(x) = 0$ at the crack tip.

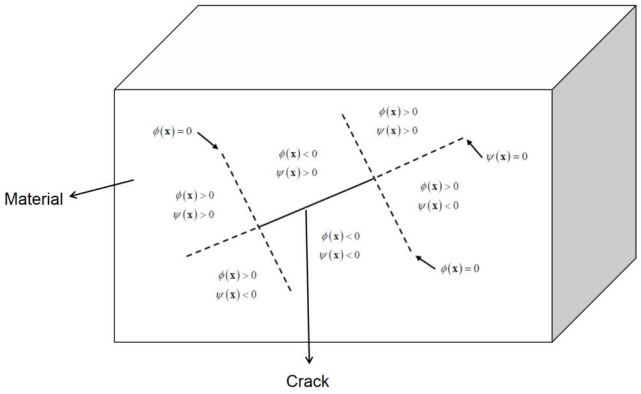

Figure.1 Extended finite element level set function symbol distribution

The displacement function of the extended finite element is based on the conventional finite element, adding the jump function and the crack tip's asymptotic displacement field function which reflect the crack surface . Taking the planar quadrilateral element as an example:

$$u(x) = \sum_i N_i(x)u_i + \sum_j N_j(x)H(x)a_j + \sum_k N_k(x)\sum_\alpha \phi_\alpha(x)b_k^\alpha \tag{5}$$

Where:

$\sum_i N_i(x)u_i$ is the displacement field function of the conventional finite element parts,whose calculation is the same as the conventional finite element;

$\sum_j N_j(x)H(x)a_j$ is the displacement field function of units penetrated by the crack;

$\sum_k N_k(x)\sum_\alpha^4 \phi_\alpha(x)b_k^\alpha$ is the displacement field function of the crack tip (edge) units;

$H(x)$ function is defined as: equal to 1 above the crack, equal to -1 below the crack.

The asymptotic displacement field function of the crack tip element is described as $\phi_\alpha(x)$.

When dealing with crack problems, the integrand is intermittent, and solving it with Gaussian integrals can cause large errors. The extended finite element method will use different points to integrate the crack elements according to the sub-regions. The crack node coordinates are determined by the zero-level set function. On the basis of the traditional finite element, the asymptotic displacement field function of the crack tip and the jump function reflecting the crack surface are added to deal with the discontinuous displacement field. Although the crack has expanded, there is no need to re-divide the mesh, which greatly reduces the computational cost.

3 Fatigue crack propagation simulation

Establish a model identical to the experiment, as shown in Figure 2, a pair of equal and large reverse pulling forces P are applied to the two circular holes. Since the applied

load is actually transmitted to the test piece by bolts, the actual stress at the bolt loading is much smaller than the stress near the crack tip with stress concentration. The non-concentrating force at the round hole has a negligible influence on the stress field at the crack tip. Considering the feasibility of modeling, the load P is the surface force acting on the surface of the circular hole and the direction does not change with the deformation.

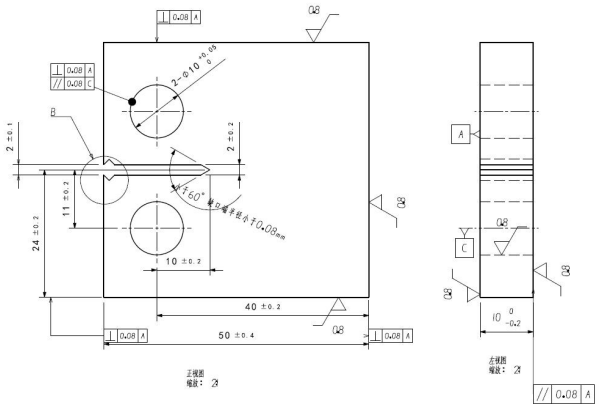

Figure.2 Inconel718 alloy unilateral notched standard CT specimen

The bayonets of the extension meter at different temperatures are different, but it is not focal point and we ignored it. Create a 3D model part identical to the test piece: Generate three new parts: Line, Crack and Plate. Plate and Line select 3D deformable solid extrusion type, Crack select 3D deformable shell extrusion type, then assemble the three parts into a whole, named Allpart, as shown in Figure 3(a)-Figure 3(d).

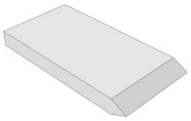

Figure 3(a) Line

Figure 3(b) Crack

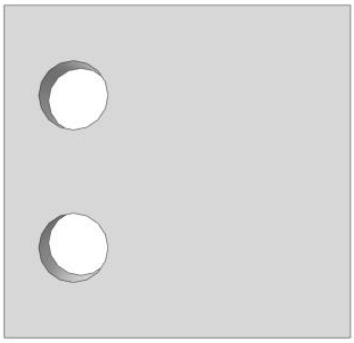

Figure 3(c) Plate

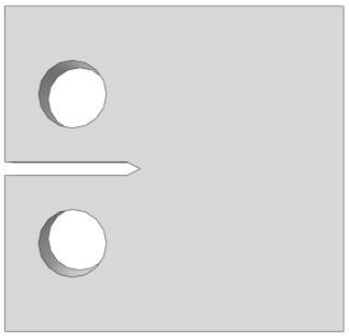

Figure 3(d) Allpart

Create the material Inconel 718 checked by the MMPDS[14], the maximum principal stress failure criterion is used as the criterion for the initiation of damage, the damage evolution is based on the energy, linear softening, mixed-mode exponential damage evolution law. The relevant parameters G1=408590MPa, G2=11000MPa, G3=30MPa[15]. The material properties for Inconel 718 obtained at different temperatures are shown in Table 1.

Temperatures (K)	Young's modulus E (M Pa)	Poisson's ratio	Maximum principal stress (M Pa)
298.15	29.0	0.293	873
573.15	26.7	0.273	842
823.15	24.7	0.283	835

Table.1 Material properties for Inconel 718

To achieve a certain accuracy of the stress intensity factor, the influence of the element on the calculation accuracy is minimized. At present, ABAQUS can only calculate the stress intensity factor of the linear element model, and the hexahedral element is selected in the crack zone. Taking into account the geometric characteristics of the model, as shown in the figure 4, the CT model components are divided into several regions.

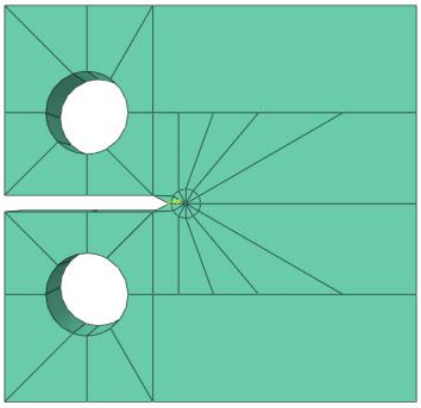

Figure.4 Model partition distribution

It is expected that the crack will expand along the upper and lower symmetry planes, and the mesh of the non-crack

extension area will be too dense or irregular to increase the calculation cost. The non-linear boundary of the non-crack extension region affects the mesh of the crack extension region, so the model is divided into several regions before meshing. In order to reduce the influence of the grid arrangement on the crack propagation path, symmetric seeds are arranged on the upper and lower relevant boundaries before and after the model to make the grid completely symmetrical.

There are three regions with different element sizes:

1.A cylindrical region centered on the pre-formed crack tip, the approximate element size is 0.08mm, use Hex-type structured element C3D8, shown in figure 5(a).

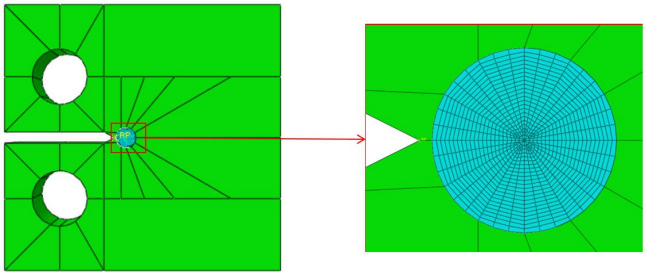

Figure 5(a) Mesh distribution of the crack tip region

2.Crack possible extension area. This area's approximate element size is 0.3 mm, use Hex-type structured element C3D8, shown in figure 5(b).

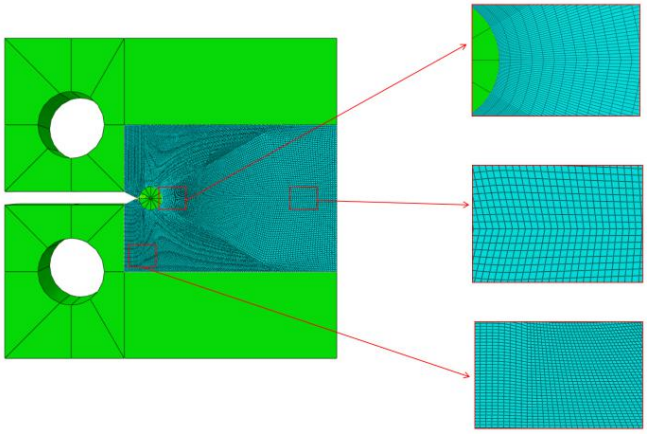

Figure 5(b) Mesh distribution of the crack extension region

3.Non-crack extension area, the calculation accuracy of this area isn't focal point, the element size is about 1 mm, use Hex-type structured element C3D8R, shown in figure 5(c).

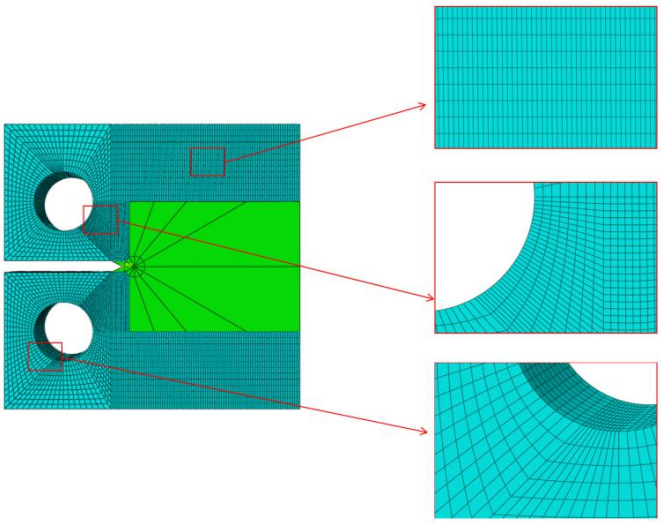

Figure 5(c) Mesh distribution of the Non-crack extension region

The whole model's total number of elements is 243160, including 44680 linear hexahedral elements of type C3D8R, 198480 linear hexahedral elements of type C3D8.shown in figure 5(d).

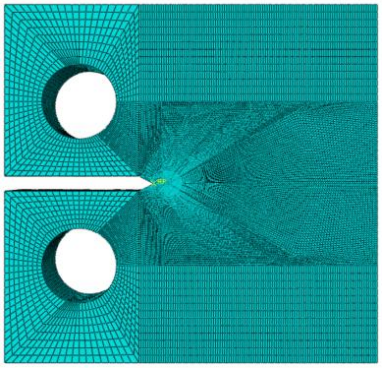

Figure 5(d) Mesh distribution of the whole model

In the interaction module, set a hard contact property, define the preset crack surface as XFEM crack in the special setting module, and don't allow the crack to expand, the model mesh will not occur with crack propagation variety.Then create a static analysis step for Step-1 and set the output of the output stress intensity factor for the crack Crack-1. To improve the accuracy, calculate the 5 cloud image integrals.

In loading module, the uniform surface loads Load-1 and Load-2 of the fixed direction (0, 1, 0) and (0, -1, 0) corresponding to Step-1 are established. Load-1 and Load-2 are respectively applied to the upper semicircular surface of the upper hole and the lower semicircular surface of the lower hole, and the values are converted to 8.8 KN; in order to make the calculation result better converge, a boundary is set at the circular hole portion. Set two boundary conditions: Condition BC-2 and BC-5's the x and z directions of the two holes are shifted to zero.

Since the load is periodic, it is necessary to define an amplitude function that is Amp-2. the loading amplitude is defined by equation (6),

$$Amp = A_0 + A_1\cos[\omega(t+t_0)] + B_1\sin[\omega(t+t_0)] \quad (6)$$

When $A_0 = 0.55, A_1 = 0, B_0 = 0.45, \omega = 31.4, t_0 = 0$

The loading stress ratio $R = \frac{(0.55-0.45)}{(0.55+0.45)} = 0.1$ was defined;

When $A_0 = 0.75, A_1 = 0, B_0 = 0.25, \omega = 31.4, t_0 = 0$

The loading stress rati $R = \frac{(0.75-0.25)}{(0.75+0.25)} = 0.5$ was defined.

Then submit the job to calculate the stress intensity factor.

After calculating the stress intensity factor, we changed the XFEM property to allow crack growth and reset the analysis step: Set up a direct loop analysis step called Step-1 in the analysis step module. The cycle period is 0.2, calculation increment is set to fixed mode, maximum incremental step is 1000000, the incremental step size is 0.02, maximum number of iterations is set to 50, and the initial value of the Fourier series term used to calculate the cyclic response is set to 20 , the maximum is set to 50, the increment is set to 5, minimum incremental step is set to 1, the maximum incremental step is set to 200, and the maximum number of cycles is set to 1000000. then set the field output variable of the analysis step Step-1 to: load at the node, node coordinates, node expansion finite element level set function PHILSM and PSILSM, node reaction force, node displacement; unit crack initiation cycle number, element strain, expansion limited Element cell state, cell stress.

Finally, the calculation is submitted to obtain the fatigue crack growth result.

4 Analysis of numerical simulation results with test results

The numerical simulation Mises stress cloud distribution under R=0.1, T=298.15K, N=135000 is shown in Fig. 6. The Magnitude cloud distribution is shown in Fig. 7. The crack propagation of other models is basically similar to Fig. 6 and Fig. 7. The crack propagates substantially along the symmetry plane of the model, and is symmetrically up and down. There is obvious Mises stress concentration at the tip of the crack and at the two holes of the model. The Mises stress of the unit near the tip of the crack propagation is the largest.

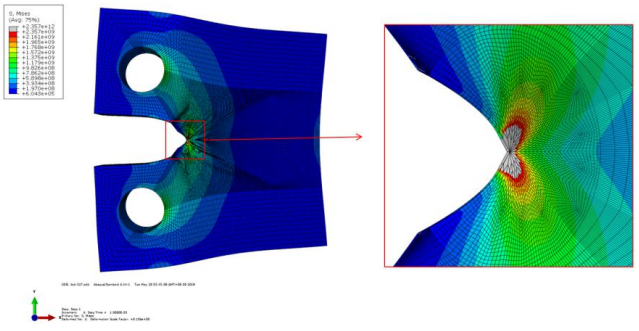

Figure 6 The Mises stress cloud distribution under R=0.1, T=298.15K, N=135000

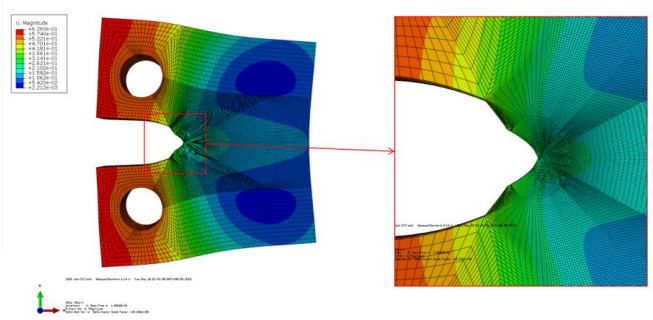

Figure 7 The Magnitude cloud distribution under R=0.1, T=298.15K, N=135000

After obtaining the data of the stress intensity factor and crack length of the output, the data of crack length and time are obtained. By scaling, we can obtain the data of fatigue crack growth rate da/dN and stress intensity factor under different conditions.

Referring to the test under the same working conditions made by the relevant departments, the scatter plot of the fatigue crack growth rate da/dN and the stress intensity factor under various conditions was obtained. According to the Paris formula[16]:

$$\frac{da}{dN} = C(\Delta K^m) \quad (7)$$

Where a is the crack length, N is the cycle time, C and m are material parameters.

Take the logarithm of the Paris formula on both sides and get:

$$\lg\left(\frac{da}{dN}\right) = \lg C + m\lg(\Delta K) \quad (8)$$

Therefore, $\frac{da}{dN}$ and ΔK have a linear relationship in the double logarithmic coordinate system. The da/dN curve of this test was determined by the test machine's own software fitting method (according to the ASTM standard). The da/dN curve data of all the test pieces were collectively collected to obtain a crack propagation curve of all the samples at each temperature in the double logarithmic coordinate system. Draw the numerical simulation curves under the same conditions in the same double logarithmic coordinate system, as shown in Figure 8(a)-Figure8(f).

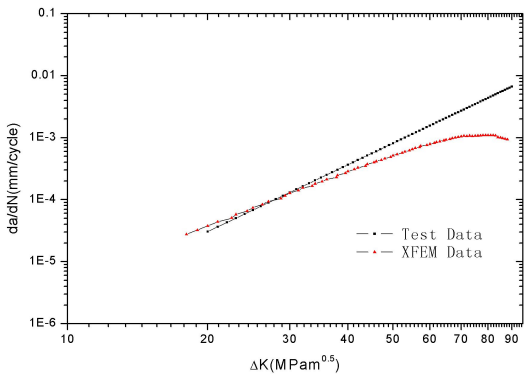

Figure 8(a) T=298.15K, R=0.1

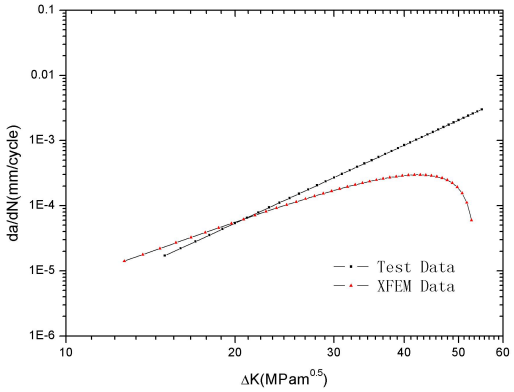

Figure 8(b) T=298.15K, R=0.5

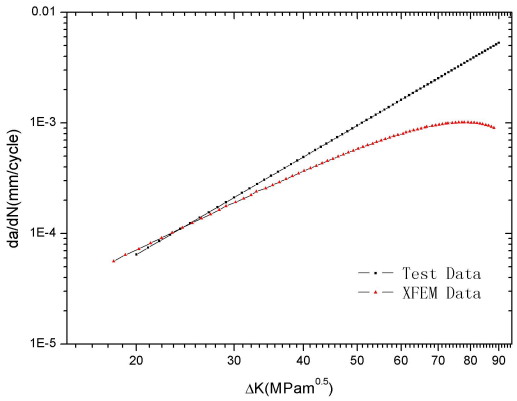

Figure 8(c) T=572.15K, R=0.1

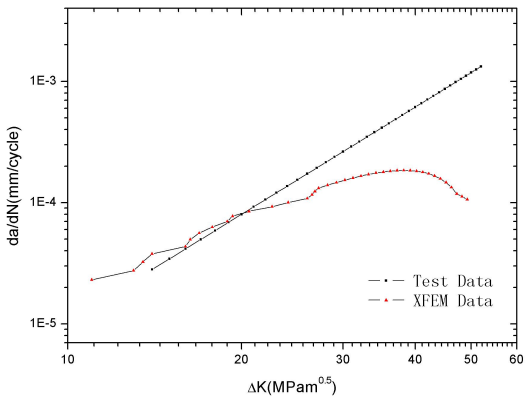

Figure 8(d) T=572.15K, R=0.5

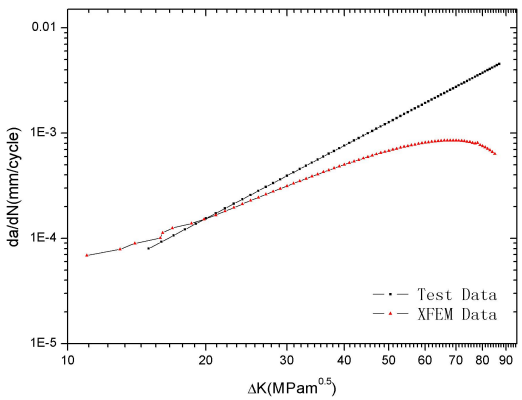

Figure 8(e) T=823.15K, R=0.1

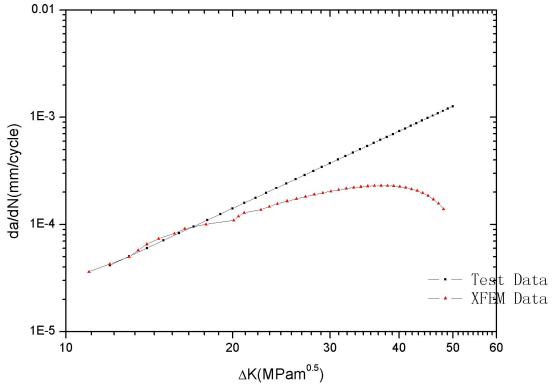

Figure 8(f) T=823.15K, R=0.5

Figure 8 Comparison of test curve and numerical simulation curve

By comparing and analyzing the theoretical prediction results and test results under six working conditions, it can be found that the theoretically predicted fatigue crack growth rate da/dN and stress intensity factor curves are relatively smooth, which is similar to the straight line obtained by the test. Most of the theoretical predictions are lower than the test results. When the stress intensity factor is small, the theoretical prediction results are relatively accurate, and the experimental results are not much different. When the stress intensity factor is large, the theoretical prediction results are significantly lower than the experimental results, because the fatigue crack propagation at this time is close to the upper boundary of the Paris region, when the number of cycles is close to the residual fatigue life, and the fatigue crack growth rate increases rapidly.

The theoretical prediction results of crack propagation length have some deviation and dispersion. This is due to the extended finite element characteristics and the fineness of the model mesh. The crack cannot be stopped inside the unit. When the crack propagation power is insufficient to cause the crack to expand beyond one unit, the crack can't expand.

5 Conclusion

1.Through the XFEM method of ABAQUS calculation software, the Inconel718 alloy unilateral notched standard CT specimen under six working conditions was numerically simulated, and the scatter plot of fatigue crack growth rate da/dN and stress intensity factor was obtained. Comparing the test results, it is found that the numerical simulation results are close to the experimental results when the stress intensity factor is small, indicating that the extended finite element method can simulate fatigue crack propagation better. Therefore, the results of numerical simulation can be used as a reference for subsequent experiments to some extent.

2.The results obtained by the extended finite element method are much lower than the experimental results when the stress intensity factor is large, and there are still many

shortcomings. For example, the crack tip cannot be stopped inside the unit, the level set function cannot define the intersecting crack, and the crack corner cannot be too large, so it is difficult to simulate the crack problem of the complicated structure. The development of fatigue fracture theory and the advancement of numerical simulation technology are waiting.

Reference

[1]垣本由紀子. (1981). 人的要因に起因する航空事故資料の分析-1-(1954-1979) コ-ド体系について. 航空医学実験隊報告, 22(3), p143-181.

[2]Lin, X. B., & Smith, R. A. (1998). Fatigue growth simulation for cracks in notched and unnotched round bars. International Journal of Mechanical Sciences, 40(5), 405-419.

[3]McClung, R. C., Chell, G. G., Russell, D. A., & Orient, G. E. (1997). A practical methodology for elastic-plastic fatigue crack growth. In Fatigue and fracture mechanics: 27th volume. ASTM International.

[4]De-Andrés, A., Pérez, J. L., & Ortiz, M. (1999). Elastoplastic finite element analysis of three-dimensional fatigue crack growth in aluminum shafts subjected to axial loading. International Journal of Solids and Structures, 36(15), 2231-2258.

[5]Yan, X. (2006). A boundary element modeling of fatigue crack growth in a plane elastic plate. Mechanics Research Communications, 33(4), 470-481.

[6]Duflot, M., & Nguyen-Dang, H. (2004). Fatigue crack growth analysis by an enriched meshless method. Journal of Computational and Applied Mathematics, 168(1-2), 155-164.

[7]Belytschko, T., & Black, T. (1999). Elastic crack growth in finite elements with minimal remeshing. International journal for numerical methods in engineering, 45(5), 601-620.

[8]Bergara, A., Dorado, J. I., Martin-Meizoso, A., & Martínez-Esnaola, J. M. (2017). Fatigue crack propagation in complex stress fields: Experiments and numerical simulations using the Extended Finite Element Method (XFEM). International Journal of Fatigue, 103, 112-121.

[9]Bhattacharya, S., Singh, I. V., Mishra, B. K., & Bui, T. Q. (2013). Fatigue crack growth simulations of interfacial cracks in bi-layered FGMs using XFEM. Computational Mechanics, 52(4), 799-814.

[10]Pathak, H., Singh, A., & Singh, I. V. (2013). Fatigue crack growth simulations of 3-D problems using XFEM. International Journal of Mechanical Sciences, 76, 112-131.

[11]Kumar, S., Singh, I. V., & Mishra, B. K. (2015). A homogenized XFEM approach to simulate fatigue crack growth problems. Computers & Structures, 150, 1-22.

[12]Kumar, M., Singh, I. V., & Mishra, B. K. (2019). Fatigue Crack Growth Simulations of Plastically Graded Materials using XFEM and J-Integral Decomposition Approach. Engineering Fracture Mechanics.

[13]Osher, S., & Sethian, J. A. (1988). Fronts propagating with curvature-dependent speed: algorithms based on Hamilton-Jacobi formulations. Journal of computational physics, 79(1), 12-49.

[14]Rice, R. C. (2003). Metallic Materials Properties Development and Standardization (MMPDS): Chapters 1-4 (Vol. 1). National Technical Information Service.

[15]Wang, R. Z., Zhang, X. C., Gong, J. G., Zhu, X. M., Tu, S. T., & Zhang, C. C. (2017). Creep-fatigue life prediction and interaction diagram in nickel-based GH4169 superalloy at 650 C based on cycle-by-cycle concept. International Journal of Fatigue, 97, 114-123.

[16]Paris, P., & Erdogan, F. (1963). A critical analysis of crack propagation laws. Journal of basic engineering, 85(4), 528-533